IOP Conf. Series: Materials Science and Engineering **818** (2020) 012012 doi:10.1088/1757-899X/818/1/012012

Development of phosphate glass and multi-phase titanate ceramic compositions for thermal treatment of irradiated nuclear fuel residues

L Harnett[1], M C Stennett[1], E R Maddrell[2] and N C Hyatt[1*]

[1]Department of Materials Science & Engineering, The University of Sheffield, Mappin Street, Sheffield, S1 3JD.
[2]National Nuclear Laboratory, Sellafield, Seascale, Cumbria, CA20 1PG, UK

*n.c.hyatt@sheffield.ac.uk

Abstract. The highly heterogeneous nature of UK legacy damaged and degraded spent nuclear fuels and so called, 'orphan fuels', prohibits the use of standard conditioning methods. An inventory of UK residual fuels yielded an account for three main fuel types: Magnox, AGR (advanced gas-cooled reactor) and MOx (mixed oxides). A series of glass and ceramic type host systems have been investigated for potential conditioning of these high uranium content spent fuel materials. Electron microscopy and powder X-ray diffraction techniques were used to characterise the prototypical wasteforms. Two sets of low-melt temperature phosphate glass compositions were trialled with additions of CeO_2 to simulate the fluorite structure and large ionic radius of U in oxide fuels. Evolution of monazite-type phases at simulant oxide fuel loadings above 15 wt.% highlighted a potential development into a glass-ceramic hybrid assemblage. Investigation into the use of an alkoxide nitrate synthesis route for SYNROC-F type ceramic precursors has allowed for the demonstration of a sintered host pyrochlore phase containing up to ~40 wt.% fuel simulant CeO_2. Gas evolution has led to increased porosity at higher temperatures and longer sintering times, this may be mitigated by higher pre-calcination temperatures.

1. Introduction

After operation in a nuclear reactor, spent fuel is retained in a storage medium, typically water, to allow for the shielding of workers from the high radiation doses and cooling of decay heat. The UK uniquely differentiates between 'damaged nuclear fuel' and 'failed' fuels: a moderate failure refers to a breach of the fuel element (such as a pinhole), whereas a damaged fuel element has a significant deviation from the typical fuel pin geometry (bent or fractured element). The severity of damaged fuel may confer conditions that can lead to processing and manipulation problems. Failed AGR (Advanced Gas cooled Reactor) fuel has historically been packed into containment using reactor-site facilities, to allow transport to ThORP (Thermal Oxide Reprocessing Plant). Pond storage of some spent fuel has led to degradation and non-conformable cladding geometry; some of this material was still reprocessed with a slightly different procedure, but the stability and integrity of a significant quantity of damaged SNF (Spent Nuclear Fuel) negates use of standard conditioning methods. In 2009, an IAEA working group

Content from this work may be used under the terms of the Creative Commons Attribution 3.0 licence. Any further distribution of this work must maintain attribution to the author(s) and the title of the work, journal citation and DOI.
Published under licence by IOP Publishing Ltd

defined damaged spent fuel as *"any SNF that requires non-standard handling to demonstrate compliance with applicable safety, regulatory or operational requirements"* [1]. Through a review of reactor-fuel specific literature and a collaborative liaison with a National Nuclear Laboratory spent fuel management team, a taxonomy of UK degraded spent fuel and fuel residues of interest was constructed. The major contributors by tons of heavy metal are: Magnox type with some Dounreay Fast Reactor breeder blanket material; low-enrichment type MOx (Mixed Oxide) fuel, steel clad AGR fuel; and a small quantity of experimental carbide fuels.

Many of the spent fuel materials in the UK inventory cannot be processed by the ThORP separation facilities, since activities terminated in 2018, and may be unsuitable for Magnox reprocessing at Sellafield before the end of its operational lifetime in 2020 [2]. Much of this legacy spent fuel is unsuitable for typical vitrification treatments due to volatile content, damage to the fuel pins, contamination through corrosion of containment, novel assembly design, experimental fuel compositions and inclusion of cutting debris [3–6]. The UK is currently considering long term disposal solutions for high activity materials in a mined Geological Disposal Facility (GDF), although very deep boreholes may prove a viable alternative [7].

2. Existing thermal treatment methods

The vast majority of studied and applied vitrification techniques focus on the addition or development of borosilicate glass (either through loading of frit or glass precursors), which can provide high chemical durability and moderate waste loading for ILW (Intermediate Level Waste) streams. However, borosilicate may be unsuitable for some HLW (High Level Waste) and orphan fuels: the poor actinide loading capability may lead to large volume increases of waste, high temperature melts could cause volatilisation of fission products, and the chemical durability may fall short for the particularly long-lived radionuclides [8]. Phosphate glasses were first investigated by the US and Germany during the 1960s, as an alternative to borosilicate: attractive for the low melt temperature and solubility of sulfates and molybdates [9]. Despite these advantages, research slowed as early phosphate glass compositions were unsuitable for waste vitrification due to: highly corrosive melts (therefore propensity to damage melters and refractories); crystallisation during annealing (nucleation of $NaPO_4$ crystallites) [10]; and devitrification at higher temperatures, leading to poor chemical durability [11]. Over the past several decades, research has returned to improving phosphate glasses for actinide waste disposition; additions of Na, Al and Fe oxides are a focus of this work since they may confer better dissolution behaviour when compared to typical borosilicate glass, with complete loading of UO_2 of at least ~12 wt.%, and melting at 1150°C [12]. This research aims to partly build upon recent work that highlighted some chemically durable SAP and SAIP (sodium-aluminium phosphate and sodium-aluminium-iron phosphate) glass compositions that are capable of ~ 49 wt.% UO_3 waste loading. Although annealing did increase crystalline development for the SAIP composition, the leach rate of U was demonstrated to be below 10 g m^{-2} d^{-1}, under PCT-B (Product Consistency Test) conditions [13].

Extensive research and development work has been carried out concerning the use of crystalline ceramic materials for the immobilisation of radioactive waste. A multiphase titanate ceramic, SYNROC (synthetic rock), has been investigated by several nuclear science institutions, in collaboration with international nuclear materials research groups [14]. One compositional variant, known as SYNROC-F was specifically designed for high UO_2 loading to directly immobilise spent fuel. The main components of this formulation are: 95 wt.% cubic U-pyrochlore type similar to betafite ($CaUTi_2O_7$) [15] for disposition of U, rare earths and Sr; up to 5 wt.% hollandite [$Ba(Al,Ti)_2Ti_6O_{16}$] [16] for immobilisation of large ionic radius radionuclides like ^{137}Cs; up to 5 wt.% tetragonal rutile or titanium dioxide (TiO_2) [17]. While synthesis has been carried out using combinations of oxides, precursors generated using sol-gel methods and proprietary techniques, further improvements could be made to streamline the preparation and improve the reactivity of SYNROC precursors, facilitating incorporation of dissolved waste and liquors.

3. Experimental methodology

3.1. Phosphate glass wasteform

The phosphate glass systems explored were based on two Fe-phosphate compositions: one with small oxide additions of Si, Al and Na, and another only with Na additions. Herein, these compositions will be referred to as IPSAS and SIP, respectively. Oxide and organic constituents were batched and homogenised with the main phosphate base as $NH_4H_2PO_4$ (98% ACS, Alfa Aesar) and Fe_2O_3 (96%, Sigma Aldrich), SiO_2 (99.5%, Alfa), Na_2CO_3 (98%, Alfa), Al_2O_3 (99%, Alfa) and CeO_2 (99.5%, Alfa). CeO_2 additions were used as an inactive simulant for UO_2, as its fluorite structure can provide suitable analogue behaviour prior to approval of active material trials. Batches were homogenised with between 0 – 20 wt.% CeO_2 as simulated spent fuel. The oxide constituents were held for 6 hours at 200°C before 2 hours at a melt temperature of 1250°C under air in an alumina crucible. Glass samples were poured onto a preheated casting plate before annealing for 4 hours at 550°C and slow cooled to room temperature. Samples from the glass coupons were ball-milled for pXRD (powder X-ray diffraction) using a Bruker D2 PHASER diffractometer with a LynxEye detector (Cu Kα, λ = 1.5418 Å radiation). Diffraction patterns were collected in fluorescence mode between $10° < 2\theta < 70°$ with a step size of 0.02° 2θ and dwell time of 3 s per step. Sections of the coupons were also mounted in resin before polishing to a 1 µm mirror finish and coated with a layer of carbon for observation by SEM (scanning electron microscopy). A Hitachi TM3030 electron microscope was coupled with a Bruker Quantax 70 EDX (energy dispersive X-ray) spectroscopy system for chemical analysis.

3.2. Multi-phase titanate wasteform

An alkoxide-nitrate synthesis method was used to generate the reactive titanate precursors. Reagents were sourced from the following: $Ca(NO_3)\cdot 4H_2O$ (99%, Acros Organics); $Ba(NO_3)_2$ (99%, Fluorochem); $Ce(NO_3)_3\cdot 6H_2O$ (99%, Sigma); $Al(OH)_3$ (98%, Acros); and $C_{12}H_{28}O_4Ti$ (96%, Fluorochem). Nitrate components were dissolved in an excess of warm de-ionised water, with the simulant waste added as $Ce(NO_3)_3\cdot 6H_2O$ for co-precipitation and ease of homogenisation. Separately, a mixture of isopropyl alcohol and aluminium hydroxide were agitated before complexing with an equal volume of titanium isopropoxide. The resulting complex was then shear mixed with the dissolved nitrates to ensure rapid and homogenous precipitation. The slurry was dried before calcining for 12 hours at 600°C, the resulting powder was ball milled to increase reactivity before uniaxial compression into pellets and sintering for 1 hour at a range of temperatures 1000°C – 1300°C. Samples were analysed by pXRD using the same instrument as in *Section 3.1* but with adjustment of the detector energy discriminator for rejection of the Fe Kα fluorescence emission from the sample for reduced background, collecting patterns between $10° < 2\theta < 55°$ with a step size of 0.02° 2θ and dwell time of 1 s per step. SEM/EDX was also conducted on the specimens using an identical method as in *Section 3.1.*

4. Results and discussions

4.1. Phosphate glass wasteform

All glasses had a high viscosity during pouring and flowed from upturned crucibles, slowing at a rate proportional to that of the increasing CeO_2 content. A coupon was successfully cast for each composition, and promptly annealed; only the 20 wt.% CeO_2 Na-Fe-phosphate glass fractured in a brittle mode after annealing. Figure 1 shows the X-ray diffraction patterns for IPSAS up to 20 wt.% CeO_2. All of the pXRD patterns demonstrated consistent diffuse scattering for $10° < 2\theta < 40°$ in both systems, indicating a disordered amorphous glass structure. At simulated fuel loadings above 10 wt.% CeO_2, minor developments of crystalline monazite ($CePO_4$, COD 9001646) [18] and cristobalite (SiO_2, COD 1010944) [19] were identified . Figure 2 is an SEM/EDX map of a SIP glass sample batched with 15 wt.% CeO_2. Light grey angular particles with diameters between 5 - 30 µm show elevated Ce detections and inclusion of P surrounding unreacted pure CeO_2. Bulk sample surfaces analysed were largely pristine, with only sporadic inclusion of partially reacted simulant waste and crystallised monazite. The glass matrices of SIP samples had an apparent saturation point for dissolution of Ce, in

the case of 15 wt.% waste SIP glass, the bulk composition by EDX had an average saturated Ce content of 9.8 ± 0.1 wt.%. However, the glass matrix local to monazite and CeO_2 crystals revealed a significantly lower average Ce component of 4.8 ± 0.5 wt.%. The bulk glass content for SIP batched with 20 wt.% CeO_2 similarly was found to have a saturated Ce component at 8.9 ± 0.1 wt.%. The waste loadings for IPSAS were not sufficient to confirm a Ce saturation point, although for the IPSAS sample batched with 20 wt.% simulant oxide waste, an average bulk glass composition of 13.1 ± 0.4 wt.% Ce was determined. Further SEM observations on this sample found comparatively less frequent instances of undigested oxide and monazite (as compared to SIP with the same waste loading).

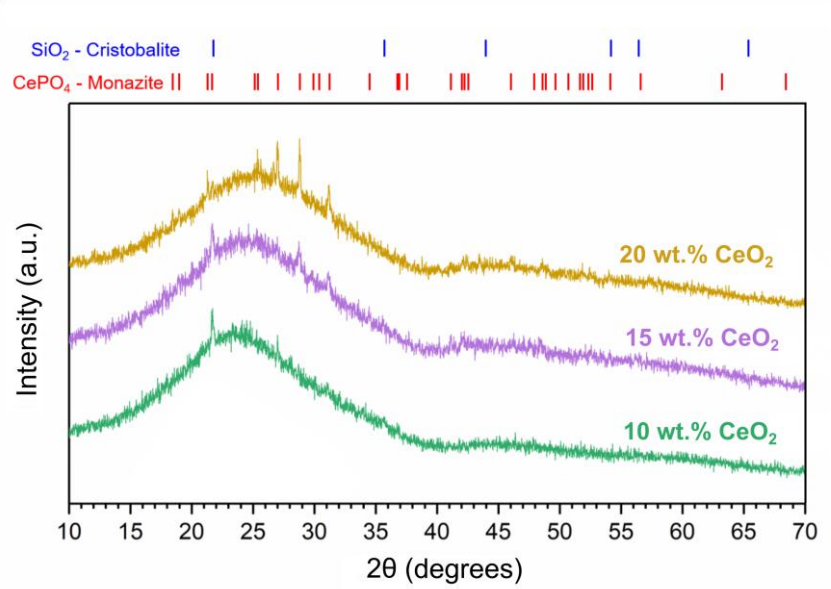

Figure 1. pXRD of IPSAS glasses 10-20 wt.% CeO_2 batches including stick patterns.

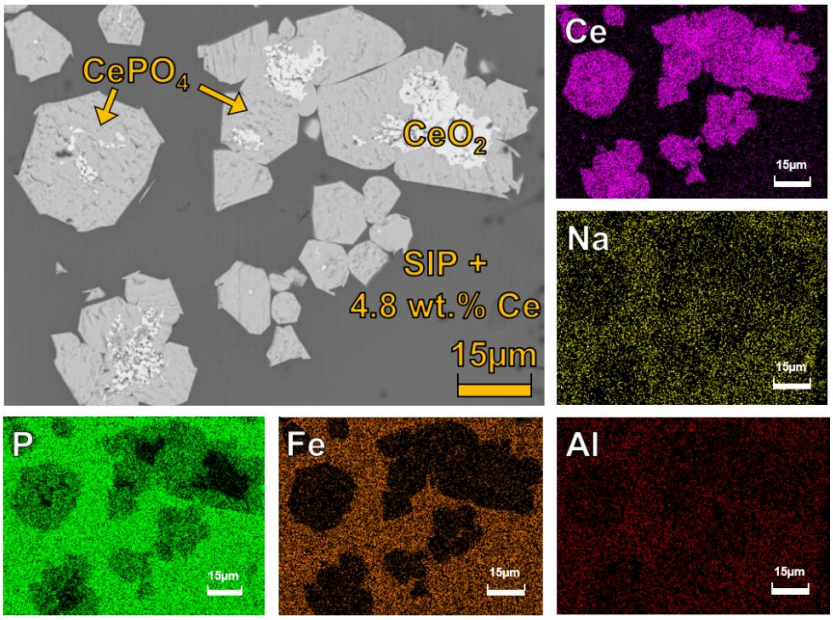

Figure 2. SEM/EDX of IPSAS glass batched with 15 wt.% CeO_2, scale-bars are 15 µm.

4.2. Multi-phase titanate wasteform

Sintering of the titanate ceramic material afforded significant pellet stability improvements, with increasing apparent hardness and darkening of colour correlating with raising the hold temperature. Figure 3 shows the pXRD patterns for the sintered pellets including data from the 600°C calcined material. The slight diffusivity of the calcined precursor indicates a moderate degree of miscibility and the presence of crystallised CeO_2 (JCPDS 78-0694) is observed. After sintering the material becomes highly crystalline, with a majority pyrochlore phase with peak positions almost identical to the U-containing equivalent pyrochlore $(Ca,Ce)_2Ti_2O_7$ ($[Ca,U]_2Ti_2O_7$, JCPDS 45-1477). A minor balance of crystalline rutile has formed and was detected for material sintered between 1000°C - 1200°C (TiO_2, JCPDS 89-0555); over the same temperature range a concomitant decrease in the relative intensity of TiO_2 and CeO_2 reflections is also evident as the phase assemblage tends towards an apparent equilibrium. However, the diffraction pattern for sample material sintered at 1300°C exhibited what appeared to be some CeO_2 reflections, a minor reflection corresponding to rutile at 40.62° 2θ, and severely diminished reflections for the pyrochlore phase. Figure 4 is a micrograph showing SEM/EDX data for the sample sintered at 1300°C. It was evident here and when analysing the bulk sample, that the light grey contrasted region with a Ce pyrochlore composition is still present as a majority primary phase. This would suggest that the titanate structure has undergone a phase transformation, to that of a new structure-type, with evolution of a gas that has led to the further development of 10 - 20 µm pores. Semi-quantitative analysis using EDX yielded an average pyrochlore composition of $(Ca_{0.57}, Ce_{0.43})_2Ti_2O_7$ (± 0.02 f.u.). Accounting for the oxygen from the CeO_2 incorporated into the structure, the approximate waste loading of this phase is ~40 wt.%. Rutile was also found (dark grey region) as a minor phase with globular morphologies.

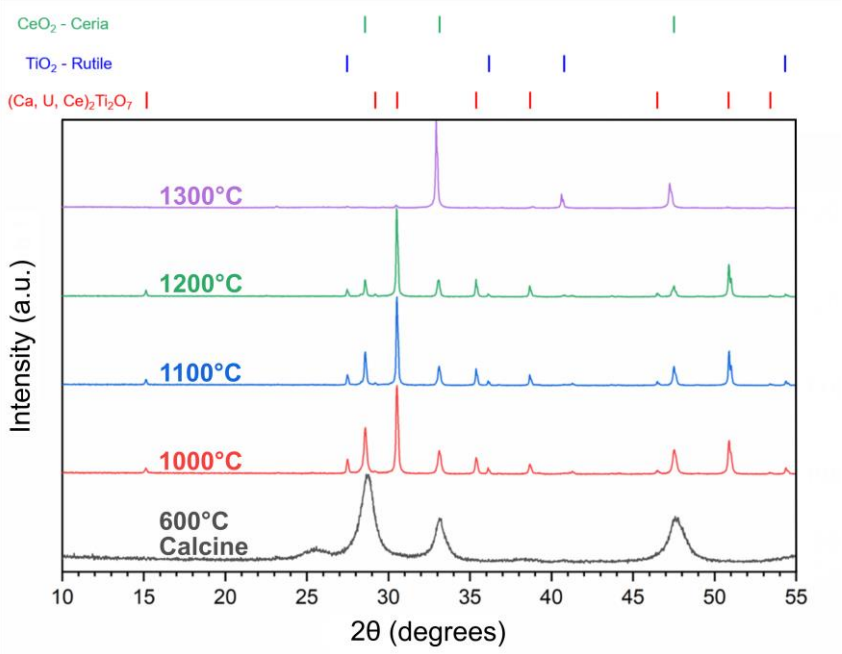

Figure 3. pXRD of co-precipitated multi-phase ceramics, as-calcined and sintered at their respective temperatures, with phase representative stick patterns.

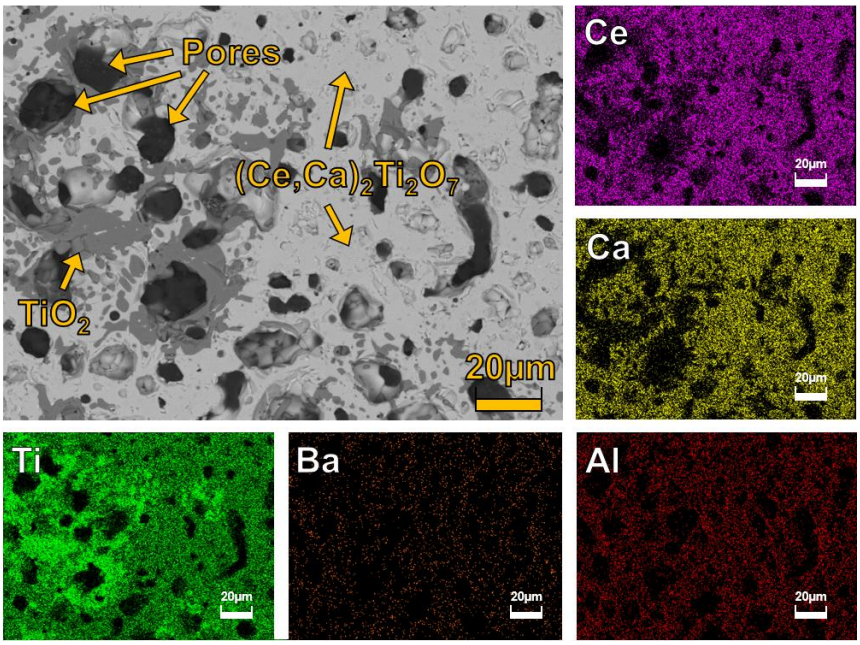

Figure 4. SEM/EDX of SYNROC-F type material cold pressed and sintered at 1300°C for 1 hour. Note Ti, Ba and Ca maps differ from Figure 2, scale-bars are 20 µm.

5. Conclusions and further work

The work conducted was able to successfully demonstrate the incorporation of CeO_2 as a waste simulant up to 13.1 ± 0.4 wt.% in a phosphate glass matrix with a quantity retained in a durable crystalline monazite phase. Further study is necessary to determine the effect of changing melt conditions, such as pressure and temperature, durability assessment by dissolution, and the coordination of Ce and Fe using XAS (X-ray absorption spectroscopy). Up to ~40 wt.% simulant CeO_2 waste was also immobilised into a pyrochlore host phase; further work will be directed at understanding structure evolution above 1200°C, generation of a hollandite secondary phase for minor actinide uptake, and durability of the wasteform.

6. References

[1] IAEA 2009 *Management of damaged spent nuclear fuel No. NF-T-3.6 Guides*
[2] Thompson G R 2014 *Radiological risk at nuclear fuel reprocessing plants*
[3] Jensen S E and Nonbol E 1998 *Description of the Magnox type of gas cooled reactor*
[4] Godfrey H 2017 *Latest understanding of corrosion of Magnox, aluminium and uranium metal wastes in cement*
[5] POST 2000 *Parliam. Off. Sci. Technol.* 1–8
[6] NDA 2011 *Exotic fuels-Dounreay Fast Reactor (DFR) breeder*
[7] NIEA 2009 *Geological disposal facilities on land for solid radioactive wastes guidance on requirements for authorisation*
[8] Sales B C and Boatner L A 1986 *J. Non. Cryst. Solids* **79** 83–116
[9] Terai R, Eguchi K and Yamanaka H 1979 *Cer. in Nucl. Wst. Mgmt.* (USDOE) pp 62–5
[10] Minaev A, Oziraner S and Prokohorova N 1979 *Cer. in Nucl. Wst. Mgmt.* (USDOE) pp 229–32
[11] Jantzen C M 1986 *J. Non. Cryst. Solids* **84** 215.
[12] Mesko M and Day D 1999 *J. Nucl. Mater.* **273** 27.
[13] Stefanovsky S V, Stefanovsky O I, Danilov S S and Kadyko M I 2019 *Ceram. Int.* **45** 9331.
[14] Ringwood A E, Kesson S E, Ware N G, Hibberson W and Major A 1979 *Nature* **278** 219.

[15] Iwata S and Cenzual K 2016 *$Ca_{1.25}U_{0.75}Ti_2O_7$ ($CaUTi_2O_7$) crystal structure.*
[16] Anthony W, Bideaux R, Bladh K and Nichols M 2005 *Handbook of mineralogy - Hollandite.*
[17] Anthony W, Bideaux R, Bladh K and Nichols M 2005 *Handbook of mineralogy - Rutile.*
[18] Yunxiang Ni, Hughes J M and Mariano A N 1995 *Am. Mineral.* **80** 21.
[19] Wyckoff R W G 1925 *Zeitschrift für Krist. - Cryst. Mater.* **62** 1.

Acknowledgement

LH is grateful to EPSRC and the Nuclear Decommissioning Authority for award of a PhD studentship. This research utilised the HADES / MIDAS Facility, established with financial support from the UK Department for Business, Energy and Industrial Strategy and EPSRC under grant reference EP/T011424/1. This research was sponsored in part by EPSRC under grant references EP/P013600/1, and EP/S01019X/1, and conducted in part under the auspices of the IAEA co-ordinated Research Programme on Management of Severely Damaged Spent Fuel and Corium (T13015) for which support is gratefully acknowledged. Statement from the authors: This paper reflects only the author's view and the European Commission is not responsible for any use that may be made of it. No potential conflict of interest was reported by the authors.